PAPER • OPEN ACCESS

Slow solar wind modeling of the Metis/Solar Orbiter – Parker Solar Probe quadrature

To cite this article: L Adhikari et al 2023 J. Phys.: Conf. Ser. 2544 012007

View the article online for updates and enhancements.

You may also like

- Influence of Large-scale Interplanetary Structures on the Propagation of Solar Energetic Particles: The Multispacecraft Event on 2021 October 9
 D. Lario, N. Wijsen, R. Y. Kwon et al.
- Prospective White-light Imaging and In Situ Measurements of Quiescent Largescale Solar-wind Streams from the Parker Solar Probe and Solar Orbiter Ming Xiong, Jackie A. Davies, Xueshang Feng et al.
- <u>2D and Slab Turbulent Cascade Rates in the Inner Heliosphere</u>
 L. Adhikari, G. P. Zank, L.-L. Zhao et al.

2544 (2023) 012007

doi:10.1088/1742-6596/2544/1/012007

Slow solar wind modeling of the Metis/Solar Orbiter – Parker Solar Probe quadrature

L Adhikari¹, G P Zank¹, D Telloni², L -L Zhao¹, and A Pitna³

³Charles University, Faculty of Mathematics and Physics, V Holešovičkách 2, 180 00 Prague 8, Czech Republic

E-mail: la0004@uah.edu

Abstract. In January 2021, Metis/SolO and PSP formed a quadrature from which the slow solar wind was able to be measured from the extended solar corona (3.5 – 6.3 $\rm R_{\odot}$) to the very inner heliosphere (23.2 $\rm R_{\odot}$). Metis/SolO remotely measured the coronal solar wind, finding a speed of 96 – 201 kms⁻¹, and PSP measured the solar wind in situ, finding a speed of 219.34 kms⁻¹. Similarly, the normalized crosshelicity and the normalized residual energy measured by PSP are 0.96 and -0.07. In this manuscript, we study the evolution of the proton entropy and the turbulence cascade rate of the outward Elsässer energy during this quadrature. We also study the relationship between solar wind speed, density and temperature, and their relationship with the turbulence energy, the turbulence cascade rate, and the solar wind proton entropy. We compare the theoretical results with the observed results measured by Metis/SolO and PSP.

1. Introduction

Since the launch of the Parker Solar Probe (PSP) and the Solar Orbiter (SolO) in 2018 and 2020 respectively, these two spacecraft have been measuring the solar wind plasma between the Sun and the Earth. During encounter 8, PSP entered a region of sub-Alfvénic solar wind for the first time [1], marking a major accomplishment of the PSP mission [2], and provided important information about turbulence near the Alfvén surface [1,3]. Similarly, the Metis coronagraph onboard the SolO [4] remotely measures the solar wind plasma in the extended solar corona [e.g., 5-7]. The dissipation of low-frequency turbulence is regarded as a promising mechanism for heating the solar corona and accelerating the solar wind [8-10, 18]. PSP and SolO provide insights on these interesting problems from an observational perspective. In addition, the PSP magnetometer [11] and plasma [12], and the SolO magnetometer [13] and plasma [14]

¹Center for Space Plasma and Aeronomic Research (CSPAR) and Department of Space Science, University of Alabama in Huntsville, Huntsville, AL 35899, USA ²National Institute for Astrophysics—Astrophysical Observatory of Torino Via Osservatorio 20, I-10025 Pino Torinese, Italy

Content from this work may be used under the terms of the Creative Commons Attribution 3.0 licence. Any further distribution of this work must maintain attribution to the author(s) and the title of the work, journal citation and DOI.

2544 (2023) 012007

doi:10.1088/1742-6596/2544/1/012007

data sets are also used to study the radial evolution of turbulence in the inner heliosphere [15,16,17].

Telloni et al [18] investigated the first alignment between PSP and SolO, when PSP was at 0.1 au at 4:00 UT on 2020-9-27, and SolO was at 1 au at 22:19 UT on 2020-10-01. Assuming ballistic propagation, Telloni et al were able to make in situ measurements of the same plasma parcel with a 1.5 hour long interval traveling from 0.1 au to 1 au. Similarly, Telloni et al [19] identified a PSP – SolO quadrature, in which the PSP during E7 was located at 0.11 au and at 18:59 UT on 2021-01-18 entered the plane of sky (POS) measured by Metis coronagraph onboard SolO on 2021-01-17 at 16:30 UT. In this case, Metis/SolO and PSP measured the same plasma parcel remotely and in situ (indicated as interval #1 in [19]) traveling from the extended solar corona $(3.3-6.3~R_{\odot})$ to the very inner heliosphere $(23.2~R_{\odot})$.

Using potential field source surface (PFSS) extrapolation [20], Telloni et al [19] found that the source region of the PSP interval #1 plasma is the equatorial extension of the southern polar coronal hole. The average solar wind speed of this interval plasma is about 219.34 kms^{-1} , and the observed normalized cross-helicity is about 0.96, indicating that this is Alfvénic slow solar wind [6,19]. Similarly, the angle between the mean magnetic field and the mean solar wind speed is measured to be $\theta_{UB} \sim 165^{\circ}$, which indicates that the observed turbulence corresponding to this interval is slab turbulence.

Adhikari et al [6] used the solar wind (SW) + NI MHD turbulence transport model equations [10] to compare the theoretical model and the joint PSP – SolO observations for the first time, from the extended solar corona to the very inner heliosphere. Adhikari et al compared the theoretical results of the solar wind speed and the solar wind density with the measured values derived from Metis/SolO and PSP, and compared the theoretical results of 2D and slab turbulence energy and the corresponding correlation lengths with the measured results derived PSP. Similarly, Biondo et al [21] modeled the PSP – SolO quadrature using the Reverse in situ and MHD Approach (RIMAP), which is a hybrid analytical-numerical method performing data-driven reconstructions of the Parker spiral. Biondo et al found good agreement between the numerical, and the Metis/SolO and PSP measured speed and density.

In this manuscript, we do not discuss the SW + NI MHD turbulence transport model equations since the model equations are presented in Adhikari et al [6]. Using the model results of Adhikari et al [6], we calculate the solar wind proton entropy and the turbulent heating rate of the outward Elsässer energy, and then consider their relationship with solar wind parameters (solar wind speed, solar wind density, and proton temperature) and the turbulence energy. Similarly, we investigate the relationship between solar wind parameters. We discuss our results in Section 2, and present a discussion and conclusions in Section 3.

2. Results

Adhikari et al [6] solved the SW + NI MHD turbulence transport model equations from $3.3~{\rm R}_{\odot}$ to $30~{\rm R}_{\odot}$ using the boundary conditions shown in Table 1. In the table, $\langle z^{\infty\pm2}\rangle$ denotes the 2D outward/inward Elsässer energy and L_{∞}^{\pm} represents the corresponding energy weighted correlation length. E_D^{∞} is the 2D residual energy and L_D^{∞} is the energy weighted correlation length of the residual energy. $\langle z^{*+2}\rangle$ is the slab outward Elsässer

2544 (2023) 012007

doi:10.1088/1742-6596/2544/1/012007

energy, and L_*^+ is the energy weighted correlation length of $\langle z^{*+2} \rangle$. U is the solar wind speed, n is the proton density, and T is the proton temperature.

2D	Values	Slab	Values	SW	Values
$\langle z^{\infty\pm 2}\rangle \; (\mathrm{km^2 s^{-2}})$	10^{5}	$\langle z^{*+2} \rangle \; (\text{km}^2 \text{s}^{-2})$	6×10^3	$U (\mathrm{km s^{-1}})$	45.13
$E_D^{\infty} (\mathrm{km^2 s^{-2}})$	2×10^3	$L_*^+ (\mathrm{km}^3 \mathrm{s}^{-2})$	9.1×10^{7}	$n (\text{cm}^{-3})$	8×10^5
$L_{\infty}^{\pm} (\mathrm{km}^3 \mathrm{s}^{-2})$	3.03×10^{9}	-	-	T(K)	7×10^5
$L_D^{\infty} (\mathrm{km}^3 \mathrm{s}^{-2})$	1.6×10^{8}	-	-	-	-

Table 1. Boundary values at 3.3 R_{\odot} for the turbulent quantities and the solar wind parameters. The same boundary condition is chosen for $\langle z^{\infty+2} \rangle$ and $\langle z^{\infty-2} \rangle$.

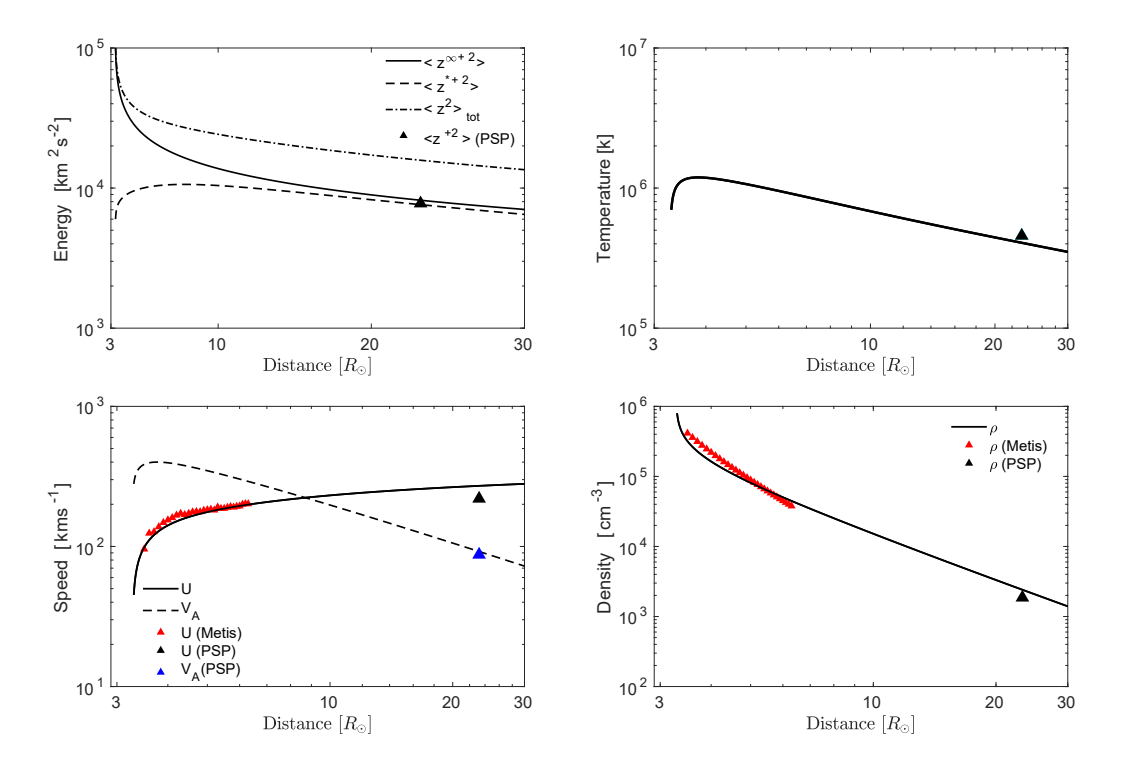


Figure 1. Comparison between the theoretical and observed outward Elsässer energy (top-left), proton temperature (top-right), solar wind speed and Alfvén velocity (bottom-left), and proton density (bottom-right) as a function of distance. The solid, dashed, and dashed-dotted-dashed curves represent the theoretical results. The red triangle denotes remotely measured speed and density by Metis/SolO (Telloni et al [19]), and the black and blue triangles denote the PSP measured values during encounter 7 (E7) (Reproduced from Adhikari et al [6]).

The top-left panel of Figure 1 displays the theoretical 2D (solid curve), slab (dashed), and 2D+slab (dashed-dotted-dashed curve), and the observed transverse (black triangle)

2544 (2023) 012007

doi:10.1088/1742-6596/2544/1/012007

25

30

outward Elsässer energy as a function of distance. Obviously, the theoretical $\langle z^{\infty+2} \rangle$ in the extended solar corona is larger than the theoretical $\langle z^{*+2} \rangle$, where $\langle z^{\infty+2} \rangle$ decreases with increasing distance ¹, while $\langle z^{*+2} \rangle$ first increases and then decreases. The dissipated turbulence energy heats the solar corona, resulting in a coronal temperature of about 10⁶ K, as shown in the top-right panel of Figure 1. The proton temperature increases abruptly from 7×10^5 K at 3.3 R_{\odot} to 1.2×10^6 K at ~ 3.75 R_{\odot}, mainly due to the dissipation of quasi-2D turbulence (see also Zank et al [9]). The hot solar corona produces a large pressure gradient that generates a large thermal force, which acts against the gravitational force, and drives the solar wind from a subsonic to a supersonic speed (bottom-left panel of Figure 1). The theoretical solar wind speed (solid curve) and the measured speed remotely by Metis/SolO (red triangles) increases rapidly between 3.3 R_{\infty} and $\sim 5 \text{ R}_{\odot}$, and then the theoretical speed increases gradually, eventually being very close to the PSP measured solar wind speed (black triangle). The theoretical Alfvén velocity (dashed curve) increases from 281 kms⁻¹ at 3.3 R_{\odot} to ~ 400 kms⁻¹ at 3.75 R_{\odot} , and then decreases monotonically with increasing distance, also being very close to the PSP measured Alfvén velocity (blue triangle). In the bottom-right panel, the theoretical proton density (solid curve) is consistent with the remotely measured proton density of Metis/SolO (red triangle) and the in situ measured proton density of PSP (black triangle).

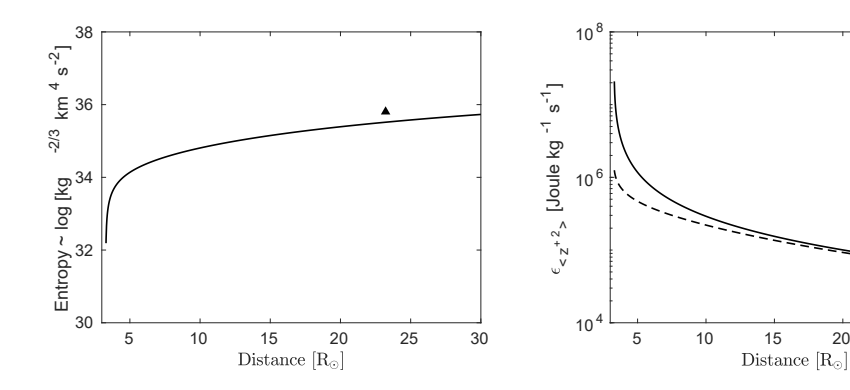


Figure 2. Left: Comparison between the theoretical (solid curve) and observed (black triangle) proton entropy as a function of heliocentric distance. Right: Comparison between the theoretical 2D (solid curve) and slab (dashed curve), and the observed (black triangle) heating rate of the outward Elsässer energy with increasing heliocentric distance.

Entropy is an important thermodynamic quantity, defined as $S = c_v \log(P/\rho^{\gamma})$, where c_v is the specific heat capacity, P is the thermal pressure, ρ is the proton mass density, and $\gamma = 5/3$ is the polytropic index. Entropy in the solar wind plasma has been studied since the late 1980s (Whang et al [22,23]). Whang et al found that, as a result of shock heating, entropy increases with distance. Recently, Adhikari et al [24] put forward the

¹ The theoretical $\langle z^{\infty-2} \rangle$ exhibits the same radial profile as that of the $\langle z^{\infty+2} \rangle$, yielding the 2D normalized cross-helicity $\sigma_c^{\infty} = 0$ from 3.3 R_O and 30 R_O (see Adhikari et al [6]).

2544 (2023) 012007

doi:10.1088/1742-6596/2544/1/012007

idea that the increase of entropy in the heliosphere is caused by turbulence dissipation. Here, we show the theoretical entropy from the extended solar corona to the very inner heliosphere, and compare with the observed entropy measured by PSP (left panel of Figure 2). Similar to the proton temperature, entropy increases rapidly within a small height from $3.3~R_{\odot}$ to $\sim 4~R_{\odot}$, which may be related to the rapid dissipation of 2D turbulence, and then increases gradually with distance.

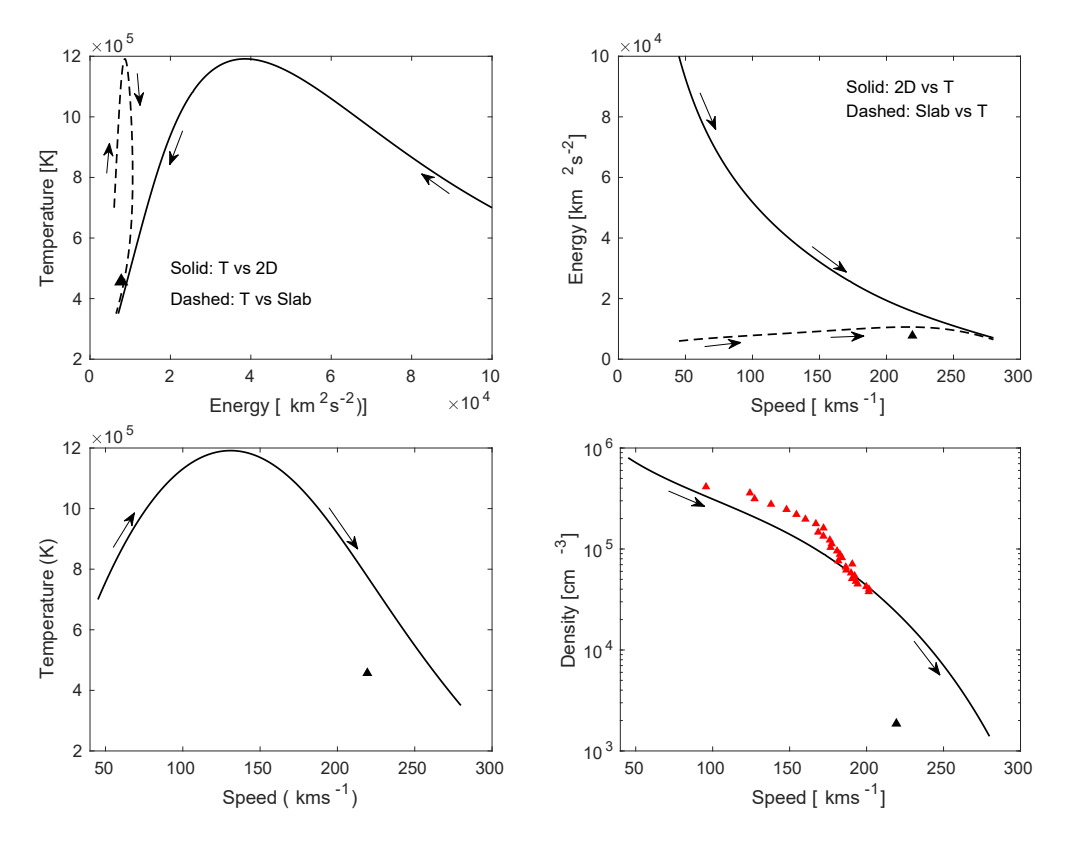


Figure 3. Top-left: Proton temperature as a function of outward Elsässer energy. Top-right: Outward Elsässer energy as a function of solar wind speed. Bottom-left: Proton temperature as a function of solar wind speed. Bottom-right: Proton density as a function of solar wind speed. The solid and dashed curves are the theoretical results. The black and red triangles are the observed results. The arrow denotes the direction from the start to end point.

A turbulence cascade simply means that the large-scale (kinetic+magnetic) energy is transferred into energy on smaller and smaller and at the very smallest scales is finally dissipated into heat energy. This is one of the well established ideas to explain the heating of the solar wind/corona. In the right panel of Figure 2, we plot the turbulent cascade rate/heating rate of the outward Elsässer energy as a function of distance. Here, the theoretical 2D (solid curve) and slab (dashed curve) turbulence cascade rates are calculated from the nonlinear dissipation terms of the 2D and slab turbulence (see [16], [25]). The observed cascade rate (black triangle) is calculated by

2544 (2023) 012007

doi:10.1088/1742-6596/2544/1/012007

 $\epsilon^+ = \langle z^{+2} \rangle^{3/2} / [C_K \log(1/k_{inj}\lambda^+)]^{3/2} \lambda^+$ (see [26]), where $\langle z^{+2} \rangle$ and λ^+ are the observed outward Elsässer energy and the corresponding correlation length, $k_{inj} = 1.07 \times 10^{-9}$ km⁻¹ is the injection wavenumber [27], and C_K is the Kolmogorov constant. We use $C_K = 4.5$. Obviously, in the extended solar corona, the theoretical 2D cascade rate is larger than the theoretical slab cascade rate, supporting the idea that 2D turbulence is the main component responsible for heating the solar corona [9].

The top-left panel of Figure 3 shows the relationship between the proton temperature and the outward Elsässer energy. The solid curve denotes the theoretical T vs $\langle z^{\infty+2} \rangle$, the dashed curve denotes the theoretical T vs $\langle z^{*+2} \rangle$, and the black triangle denotes the observed result. The arrow indicates the direction of the curve from the start point to the end point. At first, $\langle z^{\infty+2} \rangle$ is inversely proportional to T until the maximum temperature (T_{max}) , and then $\langle z^{\infty+2} \rangle$ is proportional to T. The theoretical T vs $\langle z^{*+2} \rangle$ curve shows that T and $\langle z^{*+2} \rangle$ are proportional until T_{max} , then they are inversely proportional, and then the two are directly proportional again. The theoretical T vs $\langle z^{*+2} \rangle$ curve approaches the observed result closely, in comparison to the theoretical T vs $\langle z^{*+2} \rangle$ curve. The top-right panel of Figure 3 shows that the theoretical $\langle z^{*+2} \rangle$ (solid curve) is inversely proportional to U, whereas, the theoretical $\langle z^{*+2} \rangle$ (dashed curve) is positively correlated with U until 215 kms⁻¹, close to the observed result, and then they are negatively correlated.

The bottom left panel of Figure 3 displays the relationship between the proton temperature and the solar wind speed. T and U are initially correlated until T_{max} , and then both are inversely correlated. Maksimovic et al [28] in their Figure 7, using the first orbit PSP and Helios 2 data sets, found that the proton temperature and the solar wind speed are proportional. However, in their Figures 4 and 5, they grouped the solar wind speed and the proton temperature according to the range of solar wind speeds, showing that the slow solar wind speed increases and the proton temperature decreases with distance, indicating that the proton temperature and the solar wind speed are anticorrelated, similar to our results. In a similar study, the anticorrelation between the electron temperature and the slow solar wind speed has also been observed by Halekas et al [29] using PSP measurements. In the bottom right panel of Figure 3, the theoretical (solid curve) and observed (red and black triangles) results show that the proton density decreases as a function of solar wind speed.

We plot the proton temperature as a function of proton entropy in the left panel of Figure 4. Initially, the proton temperature increases with proton entropy, and then decreases with increasing entropy. The right panel of Figure 4 shows that the proton density is anticorrelated with proton entropy, and the theoretical result is close to the observed result. This of course follows from the anti-correlated of ρ and U ($\rho Ur^2 = \text{const}$).

The top-left panel of Figure 5 shows the relationship between the 2D/slab outward Elsässer energy and the corresponding heating rate. The theoretical $\langle z^{\infty+2} \rangle$ vs $\epsilon_{\langle z^{\infty+2} \rangle}$ (solid curve) shows that the 2D outward Elsässer energy is proportional to $\epsilon_{\langle z^{\infty+2} \rangle}$. However, the theoretical $\langle z^{*+2} \rangle$ vs $\epsilon_{\langle z^{*+2} \rangle}$ (dashed curve) shows that they are initially negatively correlated, and then positively correlated. The theoretical $\langle z^{*+2} \rangle$ vs $\epsilon_{\langle z^{*+2} \rangle}$ and $\langle z^{*+2} \rangle$ vs $\epsilon_{\langle z^{\infty+2} \rangle}$ curves are close to the observed result (black triangle). In the right panel of Figure 5, the theoretical T vs $\epsilon_{\langle z^{\infty+2} \rangle}$ (solid curve) and the theoretical T

2544 (2023) 012007

doi:10.1088/1742-6596/2544/1/012007

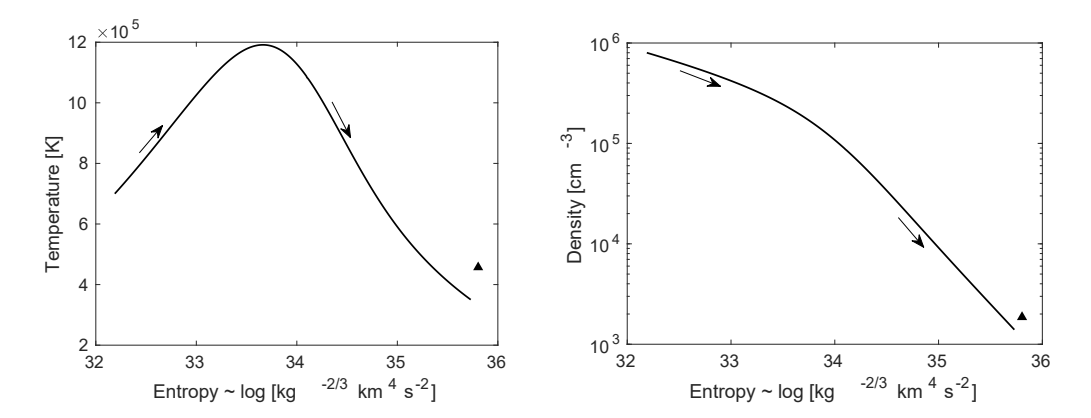


Figure 4. Left-panel: Proton temperature as a function of proton entropy. Right-panel: Proton density as a function of proton entropy. The format of the figure is similar to Figure 3.

vs $\epsilon_{\langle z^{*+2} \rangle}$ (dashed curve) show that at first T is inversely proportional to the 2D/slab heating rate, and then they are directly proportional. Finally, the bottom panel of Figure 5 shows that the solar wind speed is inversely proportional to $\epsilon_{\langle z^{\infty,*+2} \rangle}$, where the theoretical U vs $\epsilon_{\langle z^{*+2} \rangle}$ (dashed) curve steeper than the theoretical U vs $\epsilon_{\langle z^{\infty+2} \rangle}$ (solid) curve.

3. Discussion and Conclusions

Adhikari et al [6] compared the theoretical quasi-2D turbulence solar wind heating model with measurement derived from Metis/SolO – PSP quadrature investigated by Telloni et al [19]. They measured the Alfvénic slow solar wind plasma traveling from the extended solar corona $(3.5-6.3\,{\rm R}_{\odot})$ to the very inner heliosphere $(23.2\,{\rm R}_{\odot})$. The average speed of the slow solar wind measured by PSP is about 219.34 kms⁻¹ and the normalized crosshelicity is about 0.96 [6,19]. In this manuscript, we study the evolution of proton entropy and the turbulent cascade rate of the outward Elsässer energy during the Metis/SolO – PSP quadrature, and explore their relationship with the solar wind speed, solar wind density, and solar wind temperature. We summarize our findings as follows.

- (i) The theoretical solar wind proton entropy increases rapidly over a small height from $3.3~R_{\odot}$ to $\sim 4~R_{\odot}$, which may be related to the dissipation of 2D turbulence energy (e.g., Adhikari et al [24]), and then increases gradually with distance. The theoretical entropy is close to the observed entropy measured by PSP at $23.2~R_{\odot}$.
- (ii) The theoretical 2D heating rate of the outward Elsässer energy is larger than the corresponding theoretical slab heating rate in the extended solar corona. This indicates that the heating rate due to 2D turbulence is the main component for heating the solar corona.
- (iii) Initially, the theoretical proton temperature is inversely proportional to the theoretical 2D outward Elsässer energy near 3.3 R_{\odot} , and then the two are

2544 (2023) 012007

doi:10.1088/1742-6596/2544/1/012007

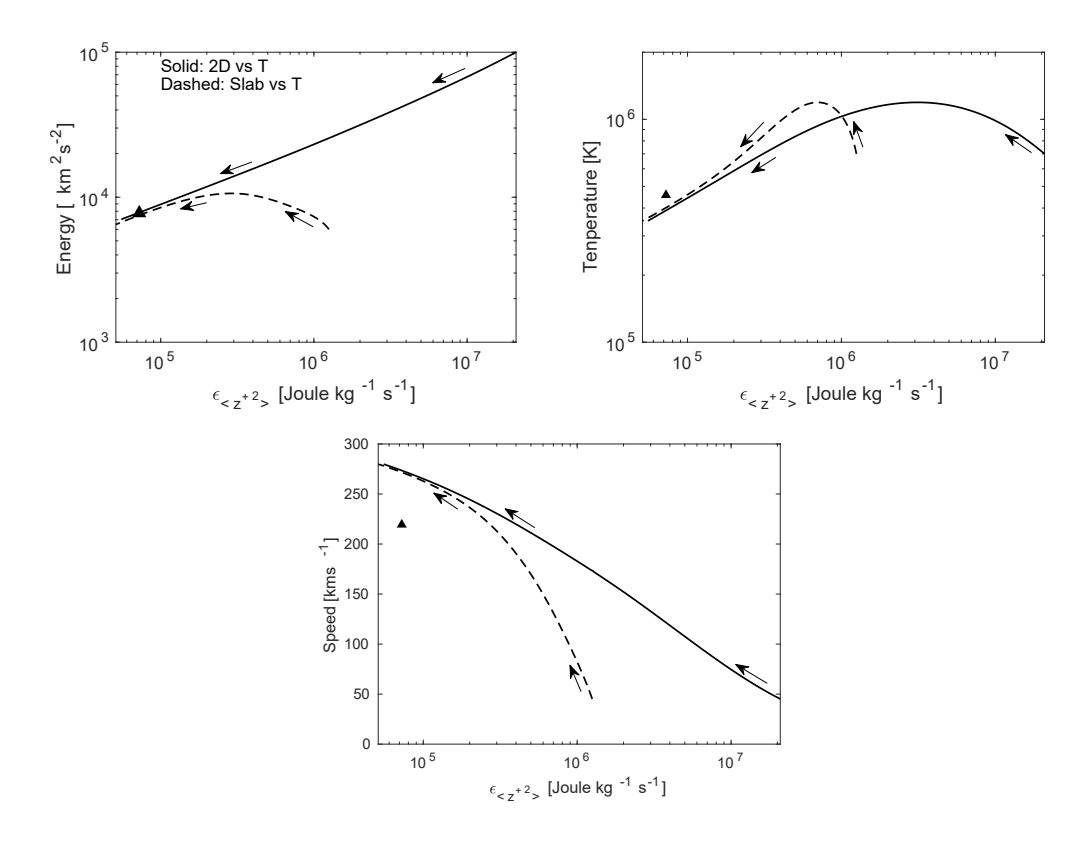


Figure 5. Top-left: Outward Elsässer energy as a function of turbulence cascade rate. Top-right: Proton temperature as a function of turbulence cascade rate. Bottom: Solar wind speed as a function of turbulence cascade rate. The format of the figure is similar to Figure 3.

proportional. Similarly, the theoretical 2D outward Elsässer energy is inversely proportional to the solar wind speed.

- (iv) The theoretical proton temperature is proportional to the theoretical solar wind speed and the theoretical proton entropy until the proton temperature reaches a maximum value, and after which the temperature is inversely proportional to them. The theoretical proton density is inversely proportional to the theoretical proton entropy.
- (v) The theoretical 2D outward Elsässer energy is proportional to the theoretical cascade rate of the 2D outward Elsässer energy.

Acknowledgments

We acknowledge the partial support of a Parker Solar Probe contract SV4-84017, an NSF EPSCoR RII-Track-1 cooperative agreement OIA-1655280, and NASA awards 80NSSC20K1783 and 80NSSC21K1319.

2544 (2023) 012007

doi:10.1088/1742-6596/2544/1/012007

References

- $[1]\,$ Kasper J C, Klein K G, Lichko E et al 2021 PhRvL127 255101
- $[2]\ \ {\rm Fox\ N\ J,\ Velli\ M\ C,\ Bale\ S\ D\ et\ al\ 2016\ \it SSRv\ 204\ 7}$
- [3] Zank G p, Zhao L L, Adhikari L, Telloni D et al 2022 ApJ, 926 9
- [4] Antonucci E, Romoli M, Andretta V et al 2020 $A \mathcal{E} A$ 642 A10
- [5] Telloni D, Zank G P, Sorriso-Valvo L et al 2022a ApJ 935 112
- [6] Adhikari L, Zank G P, Telloni D, & Zhao L L et al 2022a ApJL 937 10
- [7] Telloni D, Antonucci E, Adhikari L, Zank G P et al 2023 A&A 670 18
- [8] Matthaeus W H, Zank G P, Oughton S, Mullan D J, & Dmitruk P 1999 ApJL 523 L93
- [9] Zank G P, Adhikari L, Hunana P et al 2018 ApJ 854 32
- [10] Adhikari L, Zank G P, & Zhao L L et al 2020
a $ApJ\,901\,\,14$
- [11] Bale S D, Goetz K, Harvey P R et al 2016, SSRv 204 49
- [12] Kasper J C, Abiad R, Austin G et al 2016 SSRv 204 131
- [13] Horbury T S, O'Brien H, Carrasco Blazquez I et al 2020, A&A 642 A9
- [14] Owen C J, Bruno R, Livi S et al 2020 $A \mathcal{E} A$ 642 A16
- [15] Adhikari L, Zank G P, Zhao L L, & Telloni D et al 2022b ApJ 933 56
- [16] Adhikari L, Zank G P, Zhao L L, & Telloni D et al 2022c ApJ 938 12
- [17] Zank G P, Zhao L L, Adhikari L et al 2021 PhPl 28 080501
- [18] Telloni D, Sorriso-Valvo L, Woodham L D, Panasenco O et al 2021 ApJL 912 8
- [19] Telloni D, Zank G P, Sorriso-Valvo L et al 2022
b $ApJ\,935\,\,112$
- [20] Panasenco O, Velli M, D'Amicis R et al 2020 ApJS 246 54
- [21] Biondo R, Bemporad A, Pagano P, Telloni D et al A&A 668 5
- [22] Whang Y C, Behannon K W, Burlaga L F, & Zhang S 1989 JGR 94 2345
- [23] Whang Y C, Liu S, & Burlaga L F 1990 JGR 95 18769
- [24] Adhikari L, Zank G P, Zhao L L, & Webb G M et al 2020b ApJ 891 7
- [25] Zank G P, Adhikari L, Hunana P et al 2017 ApJ 835 147
- [26] Adhikari L, Zank G P, & Zhao L 2021 Fluid 6 368
- [27] Adhikari L, Zank G P, Telloni D et al 2017 ApJ 851 117
- [28] Maksimovic M, Bale S D, Bercic L et al 2020 ApJS 246 62
- [29] Halekas J S, Whittlesey P, Larson D E, Maksimovic E et al 2022 ApJ 936 53